Journal of ELECTRONIC MATERIALS, Vol. 41, No. 7, 2012
DOI: 10.1007/s11664-012-1999-4

Influence of Substrate Temperature on Structural Properties and Deposition Rate of AlN Thin Film Deposited by Reactive Magnetron Sputtering

HAO JIN,[1,4] BIN FENG,[1] SHURONG DONG,[1] CHANGJIAN ZHOU,[2] JIAN ZHOU,[1] YI YANG,[2] TIANLING REN,[2] JIKUI LUO,[1,3] and DEMIAO WANG[1]

1.—Department of Information Science & Electronic Engineering, Zhejiang University, Hangzhou, China. 2.—Institute of Microelectronics, Tsinghua University, Beijing, China. 3.—Centre for Materials Research & Innovation, University of Bolton, Bolton, UK. 4.—e-mail: hjin.zj@gmail.com

Aluminum nitride (AlN) thin films with *c*-axis preferred orientation have been prepared by reactive direct-current (DC) magnetron sputtering. The degree of preferred crystal orientation, the cross-sectional structure, and the surface morphology of AlN thin films grown on Si (100) substrates at various substrate temperatures from 60°C to 520°C have been investigated by x-ray diffraction, scanning electron microscopy, and atomic force microscopy. Results show that the substrate temperature has a significant effect on the structural properties, such as the degree of *c*-axis preferred orientation, the full-width at half-maximum (FWHM) of the rocking curve, the surface morphology, and the cross-sectional structure as well as the deposition rate of the AlN thin films. The optimal substrate temperature is 430°C, with corresponding root-mean-square surface roughness (R_{rms}) of 1.97 nm, FWHM of AlN (002) diffraction of 2.259°, and deposition rate of 20.86 nm/min. The mechanisms behind these phenomena are discussed. Finally, film bulk acoustic resonators based on AlN films were fabricated; the corresponding typical electromechanical coupling coefficient (k_t^2) is 5.1% with series and parallel frequencies of 2.37 GHz and 2.42 GHz, respectively.

Key words: AlN thin film, sputtering, structural properties, substrate temperature, deposition rate

INTRODUCTION

Recently, mobile communication systems have continued to acquire higher data rates and greater mobility, leading to a demand for resonators or filters with smaller sizes, higher frequencies, and wider bandwidths. Consequently, the film bulk acoustic resonator (FBAR) has been developed to meet the above demands.[1] A FBAR is composed of a piezoelectric thin film sandwiched by two electrode layers, and the key process in FBAR manufacture is the deposition of piezoelectric thin film with high quality. Aluminum nitride (AlN), zinc oxide (ZnO), and lead zirconate titanate (PZT) are the main materials for piezoelectric films. Among these, AlN has been widely used owing to its excellent characteristics such as high acoustic velocity, low acoustic loss, high thermal conductivity, and high electrical resistivity.[2,3] It is particularly important to control the crystallographic orientation of the AlN films, to obtain relatively high electromechanical coupling coefficient (k_t^2) of FBAR, because the orientation strongly affects k_t^2.[4,5]

AlN thin films have been synthesized by several methods, such as chemical vapor deposition,[6] pulsed laser ablation deposition,[7] molecular beam epitaxy,[8] the electron shower method,[9] ion beam deposition,[10]

(Received July 28, 2011; accepted February 9, 2012; published online March 8, 2012)

reactive radiofrequency (RF) magnetron sputtering,[11,12] reactive mid-frequency (MF) magnetron sputtering,[13] reactive pulsed direct-current (DC) unbalanced magnetron sputtering,[14] etc. Most of these methods can be applied to grow *c*-axis preferentially orientated AlN thin films on different substrates with suitable deposition conditions. However, reactive magnetron sputtering is a preferred choice owing to its low deposition temperature, in view of eventual integration of this technology with integrated circuit fabrication due to thermal budget limitations. In this paper, we use reactive DC magnetron sputtering[15] to deposit AlN thin film owing to its simplicity and relatively low cost.

In previous investigation, some researchers have discussed the influence of substrate temperature on the *c*-axis orientation of AlN thin film. Barshiha et al.[16] obtained a strong intensity of (002) x-ray diffraction (XRD) peak at substrate temperature of 100°C, but when the substrate temperature was between 200°C and 350°C, (100), (101), and (102) peaks appeared and the intensity of (002) decreased. On the contrary, Kao et al.[17] reported that AlN films deposited at substrate temperature below 300°C did not show any crystalline orientation, which was consistent with other researchers.[18,19] Recently, Iriarte et al.[20] found that the degree of *c*-axis orientation of AlN thin film increased with increase in substrate temperature from room temperature to 600°C. Liu et al.[21] reported that the optimal substrate temperature was 250°C rather than lower or higher substrate temperatures. Furthermore, Ababneh et al.[22] successfully deposited AlN thin films with high *c*-axis orientation on nominally unheated silicon substrates under conditions of pure nitrogen atmosphere and low sputtering pressure. Lin and Wu[23] prepared AlN thin films with high *c*-axis orientation near room temperature by use of a special buffer layer. In addition, Martin et al.[24] and Jang et al.[25] found that the *c*-axis tilted only when the substrate temperature was low enough.

Although highly *c*-axis-orientated AlN thin films were obtained at various substrate temperatures in aforementioned literature, there is still no systematic research and recognized explanation, and only a few papers have discussed the influence of substrate temperature on deposition rate.

In this work, the deposition rate and the structural properties, such as the degree of *c*-axis preferred orientation, the full-width at half-maximum (FWHM) of the rocking curve, the cross-sectional structure, and the surface morphology, of AlN thin films deposited by reactive DC sputtering were studied in detail as a function of substrate temperature.

EXPERIMENTAL PROCEDURES

All AlN thin-film samples were prepared in a planar magnetron sputter deposition system with a stainless-steel chamber which can be exhausted to minimal pressure of 5×10^{-4} Pa by a turbomolecular pump with pumping speed of 1200 L/s. The Al target with 99.999% purity and diameter of 60 mm was water-cooled. The distance between the target and the substrate was fixed at 60 mm. A thermocouple was placed on the substrate to estimate the temperature. A substrate heater assembly was attached to the holder and controlled by a proportional–integral–derivative (PID) controller, which also gave the real-time substrate temperature detected by the thermocouple. There was also a manual rotating shutter between the substrate and the target.

The polished Si (100) substrates were ultrasonically degreased and cleaned in acetone, ethanol, and deionized water for 600 s, respectively. Then they were dried by oven-baking at 100°C for 600 s. After the chamber was exhausted to 3×10^{-3} Pa, the substrate was heated to the set temperature, and then Ar gas of 99.999% purity was introduced into the chamber through a mass flow controller to presputter the Al target for 600 s prior to each AlN thin-film deposition for purification purposes. AlN thin films were grown in mixed Ar-N_2 discharges at different substrate temperatures. The purity of N_2 gas was also 99.999%, and it was also regulated by another mass flow controller. In all experiments, the deposition pressure, the Ar and N_2 gas flow, and the sputtering power were kept constant at 4.0×10^{-1} Pa, 50 sccm, 50 sccm, and 270 W, respectively. The substrate was heated by a graphite heater, and a self-heating effect of plasma was taken into account. The substrate temperature was controlled by a PID controller, which set the substrate temperature at 60°C, 160°C, 250°C, 340°C, 430°C or 520°C. The real-time substrate temperature shown on the PID controller had a maximum margin of error of ±5°C.

The FBAR devices were fabricated by bulk micromachining. A 200-nm-thick SiO_2 layer was first deposited on a Si (100) substrate. The Pt/Ti bottom electrode, about 200 nm thick, was deposited on SiO_2 and then patterned. The thickness of AlN film was about 1 μm, deposited using the optimal process. The Au/Cr top electrode was deposited with the same thickness as the bottom electrode. The resonator membrane was acoustically isolated from the supporting Si substrate by etching the latter from the backside of the wafer using a reactive-ion etching process.

The preferred crystal orientation and the FWHM were investigated by XRD, the cross-sectional structure and surface morphology were observed by scanning electron microscopy (SEM), and the surface morphology was also investigated by atomic force microscopy (AFM). An Agilent 8720ES network analyzer and a probe station were used to characterize the reflection coefficient (S_{11}) of FBAR.

RESULTS AND DISCUSSION

Deposition Rate

The degree of *c*-axis orientation of AlN thin films is thickness dependent. To obtain AlN thin

films with the same thickness in all subsequent investigations, deposition rates were measured under different substrate temperatures. Three experiments were performed to determine the deposition rates. According to the deposition rates, different sputtering time was chosen to obtain AlN thin films with thickness of about 1 μm. Figure 1 shows the effect of substrate temperature on deposition rate. From 60°C to 250°C, the deposition rate increases with substrate temperature, until the maximum rate of 21.78 nm/min is reached at 250°C. The deposition rate does not decrease monotonically above 250°C, which is different from what Chiu et al.[26] reported for substrate temperatures of 250°C and higher. Another small peak of deposition rate of 20.86 nm/min appears at 430°C.

One of the factors related to the difference of the deposition rates is the scattering of sputtering Al atoms by collisions with gases and ions. As the substrate temperature increases, it is thought that the density of gases and ions next to the substrate becomes smaller. As a result, Al atoms sputtered from the target have few chances to be scattered. Due to this decreased scattering, a greater number of particles arrive at the substrate, which contributes to the increasing deposition rate. However, there are fewer and fewer N atoms or N_2 molecules bombarding the substrate to react with Al adatoms to form AlN on the substrate according to the theory of Ishihara et al.,[27] as the amount of gases and ions reduces. For the reasons mentioned above, the deposition rate will firstly go up and then go down as the substrate temperature increases when AlN thin films are prepared in the poison regime of reactive sputtering. However, this cannot explain why there is a small peak of deposition rate for substrate temperature of 430°C. Some researchers reported that the deposition rate fell when the substrate temperature increased from 250°C to 500°C because the re-evaporation effect became stronger as the substrate temperature increased.[26] In their experiments, the energy of adatoms was much lower owing to the much higher sputtering pressure and N_2 gas flow. So, it is possible that many Al atoms re-evaporate from the surface of the AlN film before chemical reaction between Al and N atoms occurs. In our conditions, the energy of adatoms is high, but not high enough at 340°C, so the two kinds of mechanism together have the effect of reducing the deposition rate greatly. When the substrate temperature is as high as 520°C, the adatoms have enough energy to capture impinging atoms. As a result, the deposition rate will drop again at 520°C, as happened at 340°C.

Phase Analyses

Figure 2 shows the XRD patterns of samples deposited at different substrate temperatures with fixed thickness of around 1 μm. The intensity of AlN (100) peak as a function of substrate temperature is shown in the inset. The intensity of AlN (002) peak decreases to the smallest value when the substrate temperature increases from 60°C to 340°C, which is the same as was observed by Barshiha et al.[16] However, the intensity of AlN (100) peak exhibits a different trend with the same variation of substrate temperature. The intensity of AlN (100) peak decreases as the substrate temperature changes from 60°C to 250°C, while the largest value appears at 340°C. The AlN (100) peak disappears when the substrate temperature is 430°C, while the highest intensity of AlN (002) peak is observed. At this substrate temperature, the AlN thin film has a minimum FWHM of rocking curve around (002) peak of 2.259°. The intensity of AlN (002) peak decreases, and the AlN (100) peak appears again when the substrate temperature reaches 520°C, which is contrary to the results of Ivanov et al.[28]

Figures 3 and 4 show SEM cross-sectional views of the microstructure on AlN thin films deposited on Si (100) silicon under different substrate temperatures

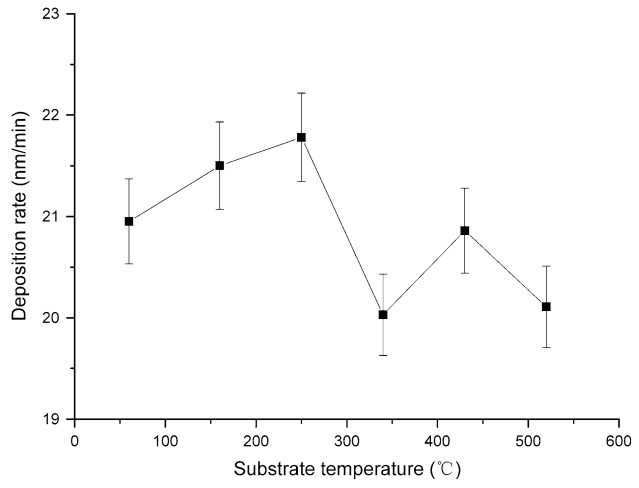

Fig. 1. Deposition rate as a function of substrate temperature.

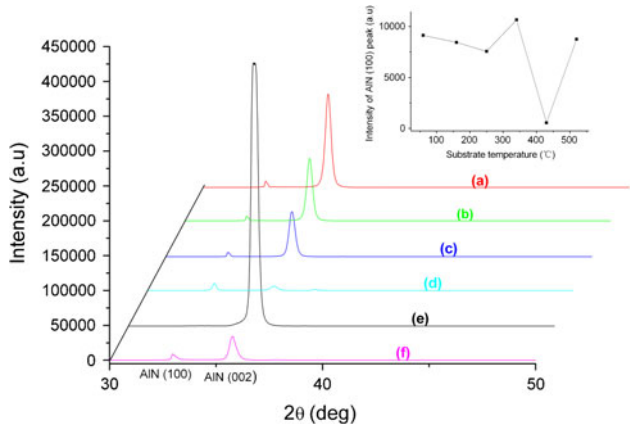

Fig. 2. XRD patterns of AlN thin films deposited at different substrate temperatures of (a) 60°C, (b) 160°C, (c) 250°C, (d) 340°C, (e) 430°C, and (f) 520°C, and the intensity of AlN (100) peak as a function of substrate temperature (inset).

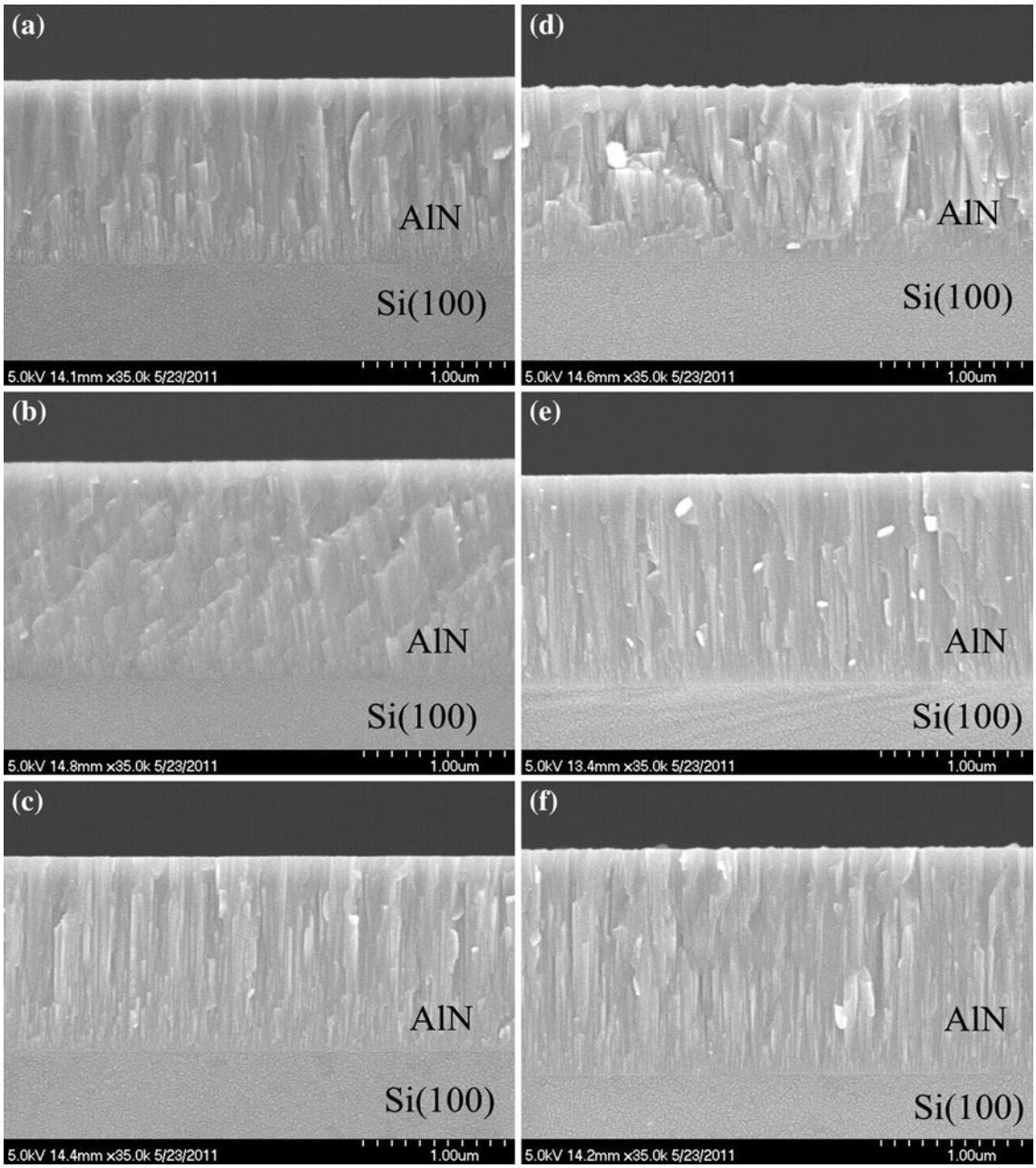

Fig. 3. SEM cross-sectional view of AlN thin films deposited at different substrate temperatures of (a) 60°C, (b) 160°C, (c) 250°C, (d) 340°C, (e) 430°C, and (f) 520°C.

and the corresponding surface morphology, respectively. All samples have columnar structure, and they are well aligned to the surface normal direction as shown in Fig. 3. However, the grain boundary intensity is quite different. The grain boundary intensity of the sample deposited at 430°C as shown in Fig. 3e is relatively low, and the columnar structure is quite uniform, while the sample deposited at 340°C has the densest grain boundary and nonuniform columnar structure as shown in Fig. 3d. Granular worm-like and spherical-droplet grains coexist in Fig. 4a–c, f. There are nonuniform facet grains in the AlN film deposited at 340°C as shown in Fig. 4d. However, only spherical-droplet grains can be found in Fig. 4e. As the substrate temperature increases from 60°C to 250°C, the ratio between granular worm-like grains and spherical-droplet grains increases, and the same trend is found when the substrate temperature increases from 430°C to 520°C.

To explain the above result, we borrowed an idea from the work of Artieda et al.,[19] who presumed that there was a threshold energy for impinging atoms and ions which determines the different growth mechanisms. We divided the results into two groups, one below 340°C and the other above 340°C,

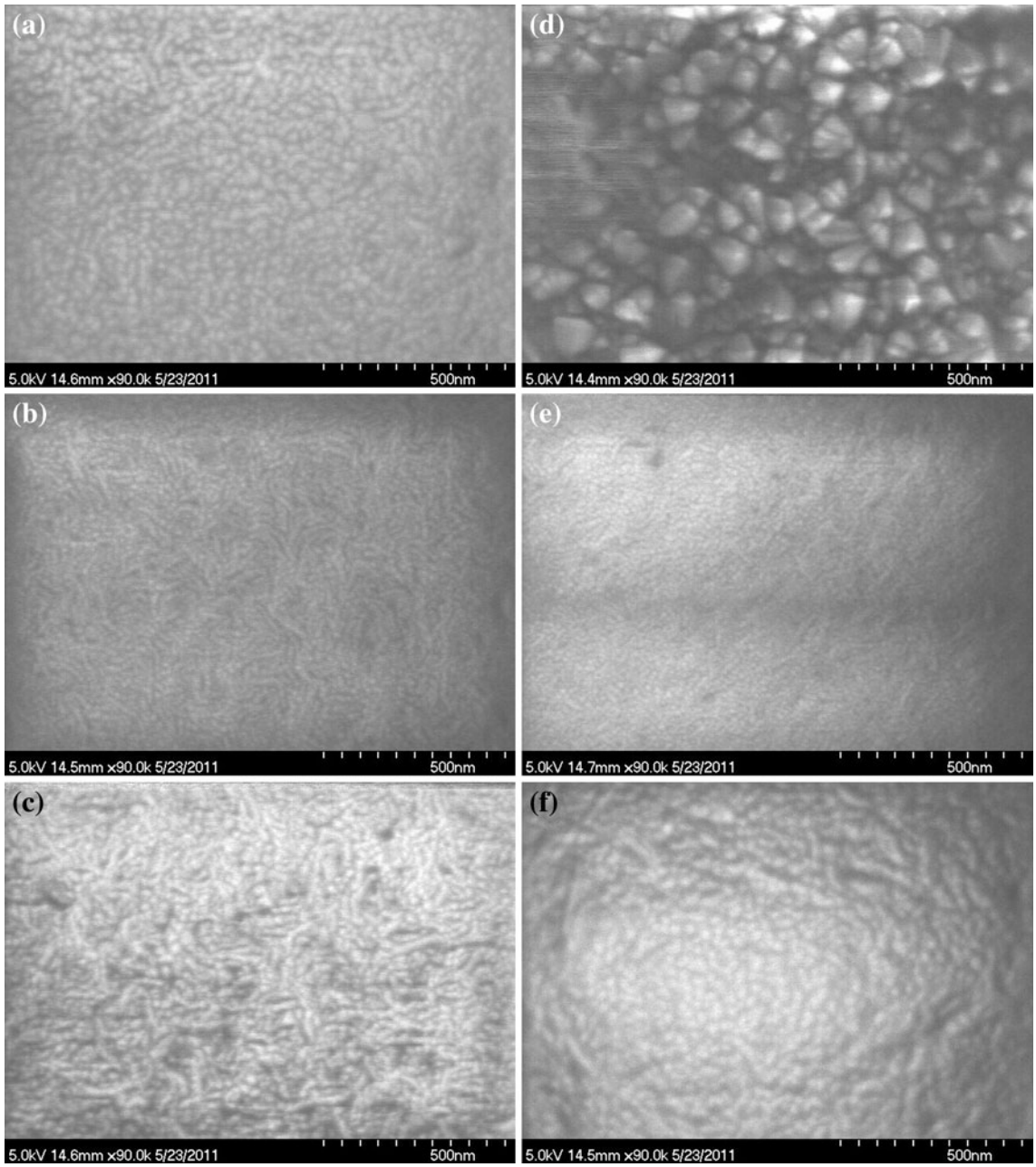

Fig. 4. SEM surface morphology of AlN thin films deposited at different substrate temperatures of (a) 60°C, (b) 160°C, (c) 250°C, (d) 340°C, (e) 430°C, and (f) 520°C.

and give explanations respectively. We assume there existed a threshold energy for adatoms, above which growth of AlN (100) plane would be suppressed and growth of AlN (002) plane would be enhanced with increasing adatom energy. On the contrary, below the threshold energy, growth of AlN (002) plane would be suppressed and grain size will increase with increasing adatom energy. As the substrate temperature increases from 60°C to 340°C, the energy of adatoms on the substrate gradually increases, but most of them do not reach or exceed the threshold energy. So, the increased energy of the adatoms due to the increasing substrate temperature will help to coarsen the grains and suppress the AlN (002) plane. This is why the intensity of AlN (002) plane decreases as shown in Fig. 2. However, the energy supplied by the substrate is quite low when the substrate temperature is below 340°C. As a result, the effect on promoting AlN (100) plane is slight, few grains become coarsened, and the nonuniformity of the grain size increases as shown in Figs. 3 and 4. This is why the peak of AlN (100) plane in Fig. 2 does not increase, but decreases slightly when the substrate temperature rises from 60°C to 250°C. When the substrate temperature increases to 340°C, most of

the grains gain enough energy to coarsen as shown in Fig. 4d, so the intensity of AlN (100) peak becomes high again. When the substrate temperature reaches 430°C, most of the adatoms exceed the threshold energy. So, the increased energy of the adatoms has been used to suppress growth of (100) plane and enhance the (002) plane, leaving little or no energy to help to coarsen the grains. Based on this reasoning, the intensity of (002) diffraction peak is much higher and no (100) peak exists in the XRD pattern of AlN thin film deposited at 430°C, and the crystal grain size shown in Fig. 4e is small and uniform. When the temperature is as high as 520°C, it is supposed that AlN thin films with excellent *c*-axis orientation and quite large and uniform crystal grains will be obtained. However, the experimental result does not show this. The reason is that the substrate temperature is too high, so that the density of gases and ions around the substrate is reduced. In other words, little energy of the sputtered Al atom is lost due to little scattering, resulting in enhanced bombardment of the substrate by energetic Al atoms and N or Ar ions, leading to crystal damage. The relative energy of adatoms decreases due to the increasing crystal damage, that is to say, the effective energy of most adatoms reduces to below the threshold energy again. For the above reasons, the (100) plane appears again at 520°C.

Figure 5 shows the trend of the surface roughness represented by the R_{rms} value of AlN thin films deposited at different substrate temperatures. The worst R_{rms} appears at 340°C and the best at 430°C, consistent with the XRD patterns. This general trend can also be explained based on the mechanism of threshold energy of adatoms mentioned above. In short, the increment of adatom energy delivered by substrate heating has two contributions: one is for grain coarsening and the other is for preferential orientation. If the overall energy of adatoms does not reach the threshold energy to suppress (100) plane growth, it will be used for grain coarsening. On the contrary, it is preferentially used to promote AlN (002) plane growth, and the rest will be used to coarsen crystal grains.

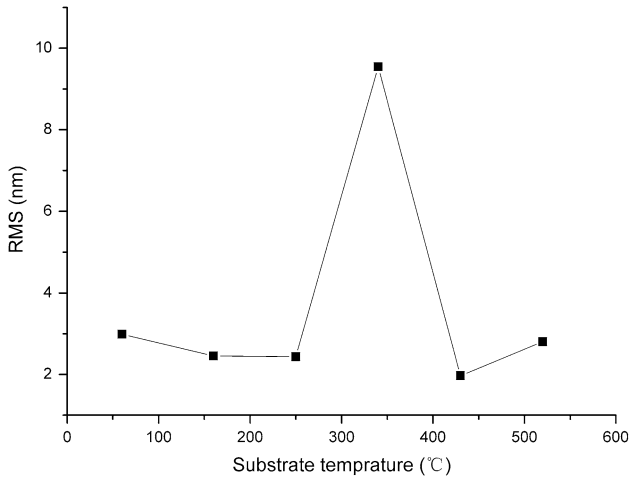

Fig. 5. Dependence of R_{rms} of AlN thin films on substrate temperature.

Electroacoustic Characterization

It is well known that better preferred *c*-axis orientation and smoother morphologies of AlN films will lead to higher k_t^2 values for FBARs.[29] We fabricated FBAR devices with the optimal deposition parameters mentioned above, and the electroacoustic characteristics were measured.

Figure 6 shows the configuration of a FBAR, which is a four-layer composite structure. The SiO_2 layer serves as a support membrane. The Ti/Pt layer acts as a nucleating layer for the oriented AlN film and also serves as the bottom electrode. The AlN film is the piezoelectric layer, and the top electrode layer is composed of Cr/Au film for bonding.

One of the fabricated FBARs is shown in Fig. 7. The k_t^2 value, which determines the maximum bandwidth that can be achieved with the FBAR devices, is evaluated by Eq. 1 from the series resonance frequency (f_s) and parallel frequency (f_p).[5]

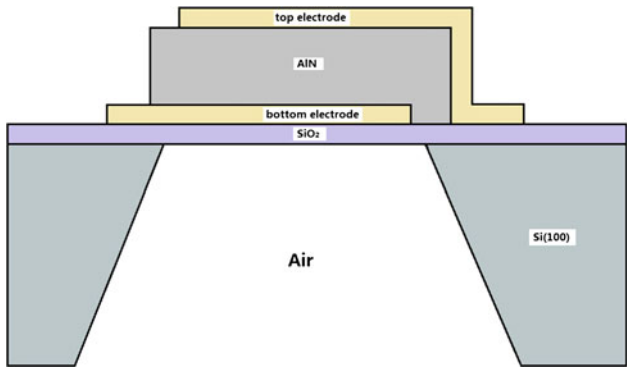

Fig. 6. Schematic of cross-section view of the FBAR.

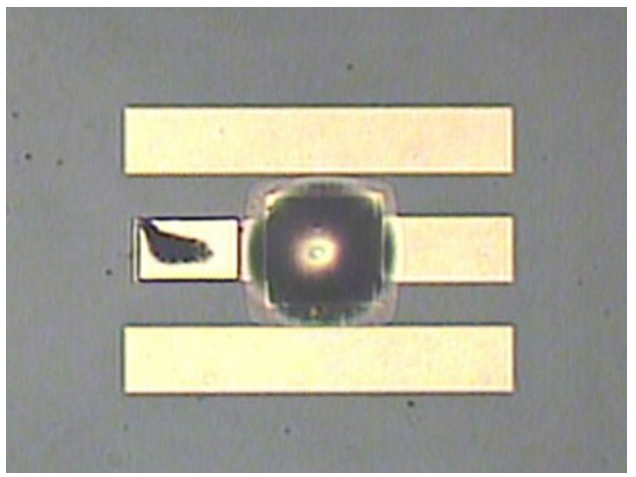

Fig. 7. Top view of the FBAR.

$$k_t^2 = \frac{(\pi/2)(f_s/f_p)}{\tan((\pi/2)(f_s/f_p))} \approx \left(\frac{\pi}{2}\right)^2 \frac{f_p - f_s}{f_p}. \quad (1)$$

Using an Agilent 8720ES network analyzer and a probe station, we obtained f_s, f_p, and k_t^2 values of 2.37 GHz, 2.42 GHz, and 5.1%, respectively. The device shows good electroacoustic characteristics.

CONCLUSIONS

We investigated the deposition rate and structural properties, such as the degree of *c*-axis preferred orientation, the FWHM of the rocking curve, the surface morphology, and the cross-sectional structure, of AlN thin films deposited by reactive DC sputtering as a function of substrate temperature in detail. Results show that the substrate temperature has a great effect on the deposition rate and the structural properties of AlN thin film. The maximum deposition rate of 21.78 nm/min was observed at 250°C due to less scattering and a proper ratio between Al and N atoms. At 430°C, we obtained AlN thin films on Si (100) substrate with the strongest intensity of AlN (002) diffraction, minimum FWHM of 2.259°, and R_{rms} of 1.97 nm. We proposed a mechanism by which the adatom energy must reach a threshold to grow with (002) preferential orientation. With the optimal process, FBAR devices were fabricated and showed good electroacoustic characteristics. The typical series resonant frequency, parallel resonant frequency, and electromechanical coupling coefficient were 2.37 GHz, 2.42 GHz, and 5.1%, respectively.

ACKNOWLEDGEMENTS

This work was supported by the National Natural Science Foundation Key Program of China (No. 60936002) and National Natural Science Foundation Program of China (No. 61171038), the Engineering and Physical Sciences Research Council (EP/F06294X/1), and The Royal Society International Joint Project with China (JP090873).

REFERENCES

1. K.M. Lakin, *IEEE Trans. Ultrason. Ferroelectr. Freq. Control* 52, 707 (2005).
2. D. Liufu and K.C. Kao, *J. Vac. Sci. Technol. A* 16, 2360 (1998).
3. S.H. Hoang and G.S. Chung, *Microelectron. Eng.* 86, 2149 (2009).
4. E. Iborra, J. Olivares, M. Clement, L. Vergara, A. Sanz-Hervas, and J. Sangrador, *Sens. Actuators A Phys.* 115, 501 (2004).
5. J. Bjurstrom, D. Rosen, I. Katardjiev, V.M. Yanchev, and I. Petrov, *IEEE Trans. Ultrason. Ferroelectr. Freq. Control* 51, 1347 (2004).
6. Y.A. Xi, K.X. Chen, F. Mont, J.K. Kim, E.F. Schubert, C. Wetzel, W. Liu, X. Li, and J.A. Smart, *J. Electron. Mater.* 36, 533 (2007).
7. S.S. Hullavarad, R.D. Vispute, B. Nagaraj, V.N. Kulkarni, S. Dhar, T. Venkatesan, K.A. Jones, M. Derenge, T. Zheleva, M.H. Ervin, A. Lelis, L.J. Scozzie, D. Habersat, A.E. Wickenden, L.J. Currano, and M. Dubey, *J. Electron. Mater.* 35, 777 (2006).
8. G. Kipshidze, S. Nikishin, V. Kuryatkov, K. Choi, I. Gherasoiu, T. Prokofyeva, M. Holtz, H. Temkin, K.D. Hobart, F.J. Kub, and M. Fatemi, *J. Electron. Mater.* 30, 825 (2001).
9. M. Ishihara, H. Yumoto, T. Tsuchiya, and K. Akashi, *Thin Solid Films* 282, 321 (1996).
10. T.L. Hu, S.W. Mao, C.P. Cha, M. Wu, H.L. Huang, and D. Gan, *J. Electron. Mater.* 36, 81 (2007).
11. J.B. Lee, J.P. Jung, M.H. Lee, and J.S. Park, *Thin Solid Films* 447, 610 (2004).
12. J. Xiong, H.S. Gu, W. Wu, M.Z. Hu, P.F. Du, and H. Xie, *J. Electron. Mater.* 40, 1578 (2011).
13. H.E. Cheng, T.C. Lin, and W.C. Chen, *Thin Solid Films* 425, 85 (2003).
14. F. Martin, M.E. Jan, B. Belgacem, M.A. Dubois, and P. Muralt, *Thin Solid Films* 514, 341 (2006).
15. H.C. Seo, I. Petrov, and K. Kim, *J. Electron. Mater.* 39, 1146 (2010).
16. H.C. Barshiha, B. Deepthi, and K.S. Rajam, *Thin Solid Films* 516, 4168 (2008).
17. K.S. Kao, C.C. Cheng, and Y.C. Chen, *IEEE Trans. Ultrason. Ferroelectr. Freq. Control* 49, 345 (2002).
18. T.T. Leung and C.W. Ong, *Diam. Relat. Mater.* 13, 1603 (2004).
19. A. Artieda, M. Barbieri, C.S. Sandu, and P. Muralt, *J. Appl. Phys.* 105, 0245042 (2009).
20. G.F. Iriarte, J.G. Rodriguez, and F. Calle, *Mater. Res. Bull.* 45, 1039 (2010).
21. W.J. Liu, S.J. Wu, C.M. Chen, Y.C. Lai, and C.H. Chuang, *J. Cryst. Growth* 276, 525 (2005).
22. A. Ababneh, U. Schmid, J. Hernando, J.L. Sanchez-Rojas, and H. Seidel, *Mater. Sci. Eng. B Adv. Funct. Solid-State Mater.* 172, 253 (2010).
23. Y.R. Lin and S.T. Wu, *Surf. Sci.* 516, L535 (2002).
24. F. Martin, M.E. Jan, S. Rev-Mermet, B. Belgacem, D. Su, M. Cantoni, and P. Muralt, *IEEE Trans. Ultrason. Ferroelectr. Freq. Control* 53, 1339 (2006).
25. H.W. Jang, H.C. Kang, D.Y. Noh, and M.S. Yi, *J. Appl. Phys.* 94, 2957 (2003).
26. K.H. Chiu, J.H. Chen, H.R. Chenc, and R.S. Huang, *Thin Solid Films* 515, 4819 (2007).
27. M. Ishihara, S.J. Li, H. Yumoto, K. Akashi, and Y. Ide, *Thin Solid Films* 316, 152 (1998).
28. I. Ivanov, L. Hultman, K. Jarrendahl, P. Martensson, J.E. Sundgren, B. Hjorvarsson, and J.E. Greene, *J. Appl. Phys.* 78, 5721 (1995).
29. C.L. Huang, K.W. Tay, and L. Wu, *Solid-State Electron.* 49, 219 (2005).